Biophysical Journal, Volume *120*

Supplemental Information

Multistep Changes in Amyloid Structure Induced by Cross-Seeding on a Rugged Energy Landscape

Keisuke Yuzu, Naoki Yamamoto, Masahiro Noji, Masatomo So, Yuji Goto, Tetsushi Iwasaki, Motonari Tsubaki, and Eri Chatani

Supplemental Methods

CD spectroscopy.

CD spectra were recorded using a J-1100 spectropolarimeter (JASCO, Tokyo, Japan). Sample solutions were prepared at a protein concentration of 0.2 mg/mL in 25 mM HCl for native insulin and 0.2 mg/mL in 25 mM HCl containing 100 mM NaCl for fibril samples, and in the measurement of amyloid fibrils, the sample was sonicated to improve dispersibility. Each scan was performed at 20 nm/min from 250 to 196 nm with a 0.1 cm path-length quartz cell. All spectra were obtained from the integration of five individual scans and expressed as mean residue molar ellipticity [θ] in monomer unit.

Purification of A-chain and B-chain.

A-chain and B-chain were obtained from human insulin. A-chain was purified as described previously (1) with a slight modification. Human insulin was dissolved at a concentration of 5.0 mg/mL in 50 mM sodium phosphate buffer (pH 7.4) containing 1 mM ethylenediaminetetraacetic acid and 10 mM dithiothreitol. After overnight incubation at 25 °C, the solution was centrifuged at 1,800 ×g for 30 min and A-chain in the supernatant was separated, and then solvent exchange with Milli-Q water was performed using a PD-10 column. B-chain was purified as described in our previous report (2). The A-chain and B-chain concentrations were determined using absorption coefficients of 1.07 $(mg/mL)^{-1}$ cm^{-1} and 0.90 $(mg/mL)^{-1}$ cm^{-1} at 280 nm (1, 2), respectively.

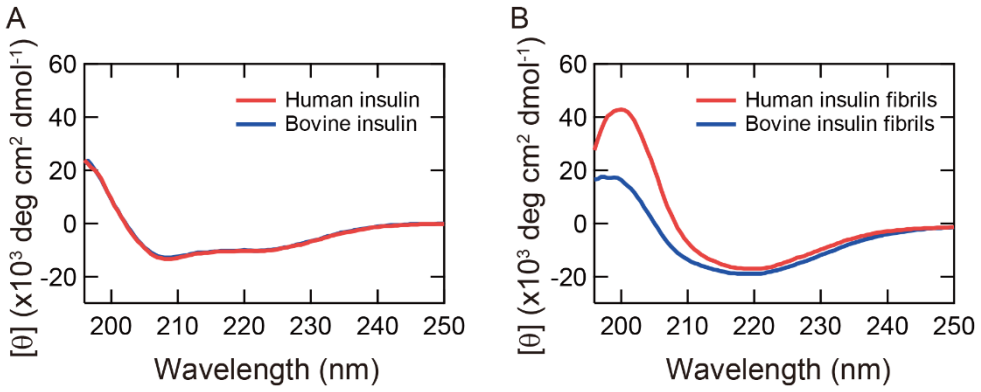

Figure S1. Far-UV CD spectra of human and bovine insulin in (A) native and (B) fibrillar states. In panel B, the same amyloid fibrils investigated in Figure 1 were subjected to the CD measurements.

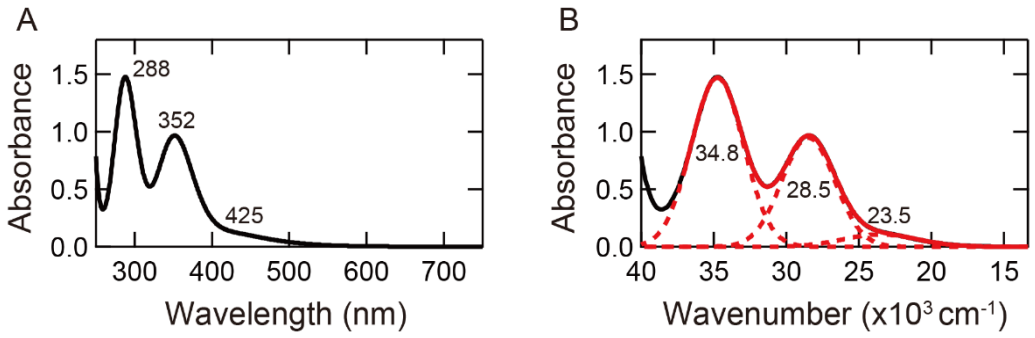

Figure S2. UV-Vis spectrum (A) and its deconvolution (B) of an iodine solution. An iodine solution containing 0.9 mM KI and 0.12 mM I_2 in 25 mM HCl was used for the measurement. A black line represents the experimental spectrum, and a red line represents the fitted spectrum using eq. 1 assuming three Gaussian bands (i.e., $n = 3$). Three Gaussian peaks are represented with dashed red lines, which correspond to absorption components obtained by the deconvolution. The Gaussian bands at 288 nm (35×10^3 cm^{-1}) and 352 nm (29×10^3 cm^{-1}) were assigned to I_3^-, and that at 425 nm (24×10^3 cm^{-1}) was assigned to I_2 (3).

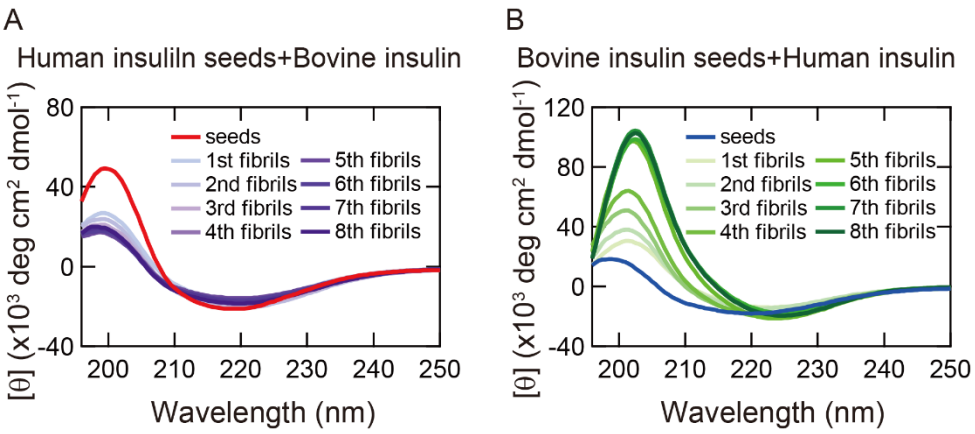

Figure S3. Far-UV CD spectra of (A) bovine insulin cross-seeded with human seeds and (B) human insulin cross-seeded with bovine seeds. The same amyloid fibrils investigated in Figure 4 were subjected to the CD measurements.

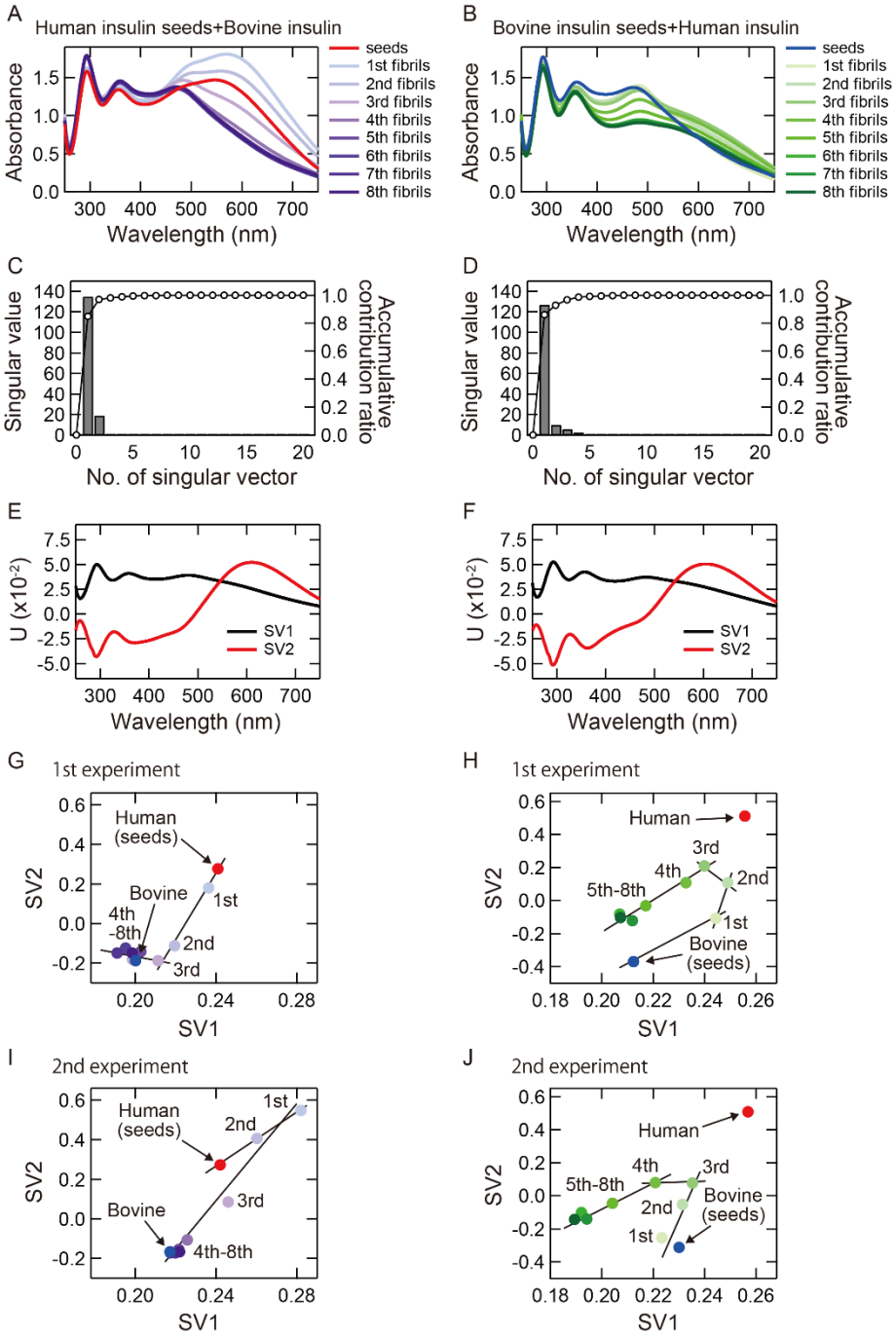

Figure S4. Reproducibility of SVD analysis of UV-Vis absorption spectra obtained from iodine-stained insulin fibrils formed by cross-seeding. To examine the reproducibility of the placement of points and the line segments on the SVD diagram, an additional SVD analysis was performed for each type of cross-seeding using a newly obtained dataset in addition to the original one. (A, B) UV-Vis absorption spectra of iodine-stained bovine (A) and human insulin fibrils (B) formed by cross-seeding. The datasets in panels A and B, respectively were subjected to SVD analysis together with the original ones shown in Figure 4D, E, respectively. Before the analysis, the intensity of the two independent datasets was normalized based on the peak intensity around 295 nm

of the seeds. (C, D) The diagonal element of the singular matrix for the datasets of bovine insulin seeded with human seeds (C) and those of human insulin seeded with bovine seeds (D). (E, F) The 1st (SV1) and 2nd (SV2) columns of the left-singular matrix of bovine insulin seeded with human seeds (E) and human insulin seeded with bovine seeds (F). Both of the results showed two dominant singular vectors SV1 and SV2 similar to those shown in Figure 6B. (G-J) Transition diagrams obtained by plotting scores of the 1st (SV1) and 2nd (SV2) rows of the right-singular matrix of bovine insulin seeded with human seeds (G, I) and human insulin seeded with bovine seeds (H, J). Solid lines were superimposed in all panels to estimate the number of transitions.

As shown in panels H and J, the transition diagram of human insulin seeded with bovine seeds successfully reproduced the characteristic U-shaped route with similar placements of the plots, and the formation of the same new-type fibrils was also confirmed. However, regarding the number of line segments, only three line segments were identified in panel J and it was difficult to conclude the exact number of intermediate metastable states that pass through during the cross-seeding process.

In the case of bovine insulin seeded with human seeds, significant differences in the placement of the plots were observed between panels G and I, failing to reproduce the same route of the structural transitions. Nevertheless, the plots were composed of two line segments. It was also demonstrated that fibril structure changed to the intrinsic fibril structure of bovine insulin after multistep structural changes. Although the pathways were diverse, it was finally concluded that the structural changes proceed with a two-step structural transition through an intermediate metastable state.

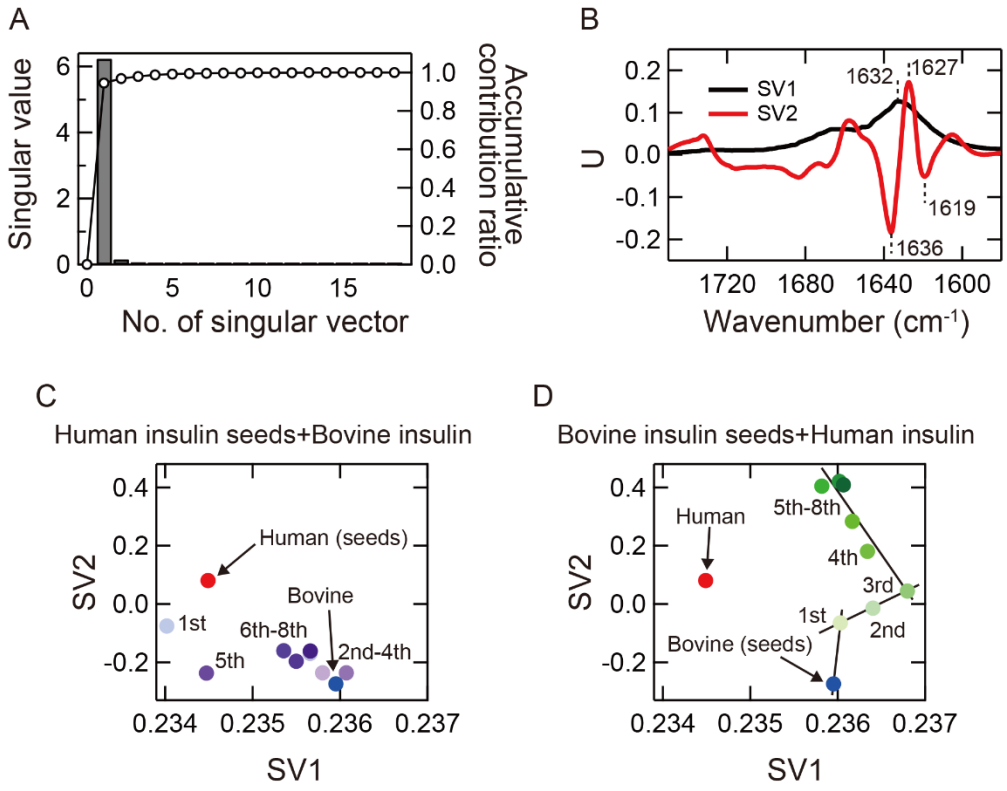

Figure S5. SVD analysis of ATR-FTIR spectra obtained from insulin fibrils formed by cross-seeding. The SVD analysis was performed with the FTIR spectra observed in the repeated cross-seeding shown in Figure 4B, C. (A) The diagonal element of the singular matrix. (B) The 1st (SV1) and 2nd (SV2) columns of the left-singular matrix. The positions of main peaks at around 1630 cm^{-1} indicative of β-sheet structures are labeled in the graphs. (C, D) Transition diagrams obtained by plotting scores of the 1st (SV1) and 2nd (SV2) rows of the right-singular matrix. The plots in the transition diagrams were more scattered than those of iodine staining due to small changes in FTIR spectra, making it relatively difficult to capture intermediate states especially in the cross-seeding of bovine insulin with human seeds (C). Nevertheless, the transition diagram of the cross-seeding of human insulin with bovine seeds showed systematic changes in plots which could be represented by the combination of multiple linear segments (D). In this plot, the most of the intermediates identified in Figure 6 were found, except for one in the 1st–3rd generations. The partial success in the SVD analysis of the FTIR spectra suggests that the multistep structural transitions could also be detected at the secondary structure level. It is tempting to find a clear correlation in singular vectors between FTIR spectra and iodine staining; however, this could not be achieved only with the present experimental data.

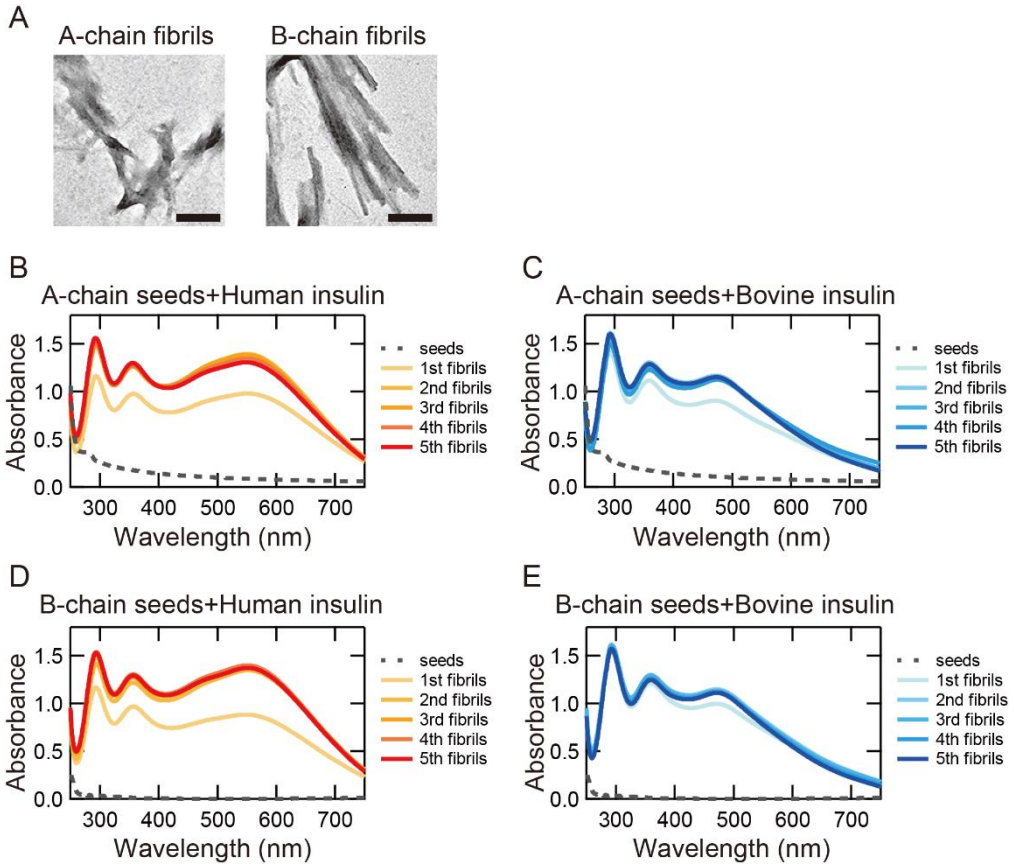

Figure S6. Cross-seeing of human/bovine insulin using human A-chain and B-chain fibrils as seeds. (A, B) TEM images of A-chain (A) and B-chain fibrils (B). The black scale bars represent 200 nm. (C–F) UV-Vis absorption spectra of iodine-stained human and bovine insulin cross-seeded with A-chain (C, D) or B-chain fibrils (E, F). Seeding reaction was performed under the same conditions as used for the cross-seeding with human or bovine insulin fibrils as seeds in Figure 4. The incubation time was set to 18 h for each cycle of cross-seeding except for the first cycle, where the incubation time was changed to 100 h because the reaction speed was much slower. Iodine staining was performed by using the same protocols as used for the self- and cross-seeding with human or bovine insulin fibrils as seeds in Figures 3 and 4. As shown by dashed lines in (C) and (D), A-chain and B-chain fibrils themselves showed little absorption even after mixing with iodine solution, probably due to the disruption of polyiodide ions by their reduction by free thiol groups of cysteine residues in A-chain and B-chain fibrils. The UV-Vis absorption spectra showed a similar shape to those of the self-seeding of human and bovine insulin, respectively (see Figure 3D, E), demonstrating that A-chain and B-chain fibrils did not work as a template.

Supporting References

1. Hong, D. P., A. Ahmad, and A. L. Fink. 2006. Fibrillation of human insulin A and B chains. *Biochemistry.* 45:9342-9353.
2. Yamamoto, N., S. Tsuhara, A. Tamura, and E. Chatani. 2018. A specific form of prefibrillar aggregates that functions as a precursor of amyloid nucleation. *Sci. Rep.* 8:62.
3. Hiramatsu, T., N. Yamamoto, S. Ha, Y. Masuda, M. Yasuda, M. Ishigaki, K. Yuzu, Y. Ozaki, and E. Chatani. 2020. Iodine staining as a useful probe for distinguishing amyloid fibril polymorphs. *Sci. Rep.* 10:16741